A

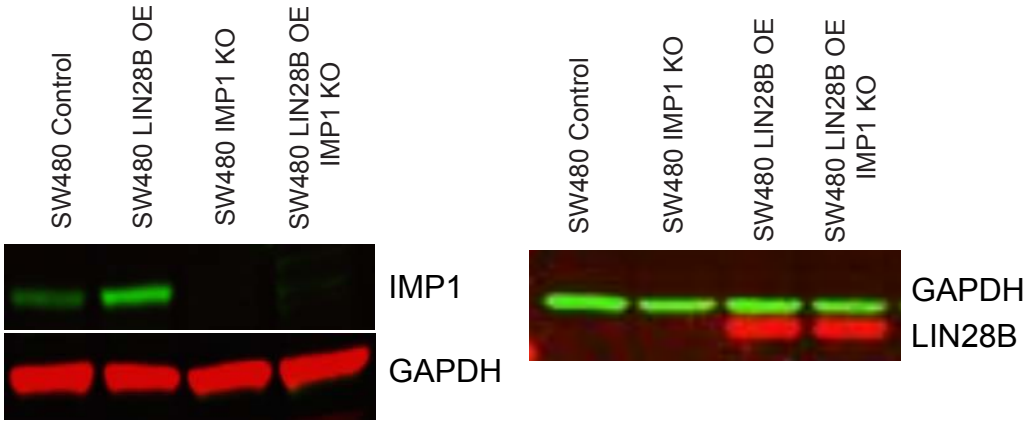

B

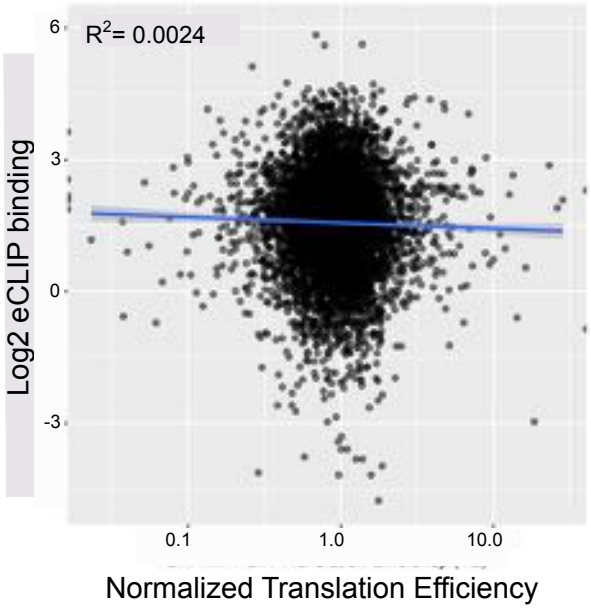

C

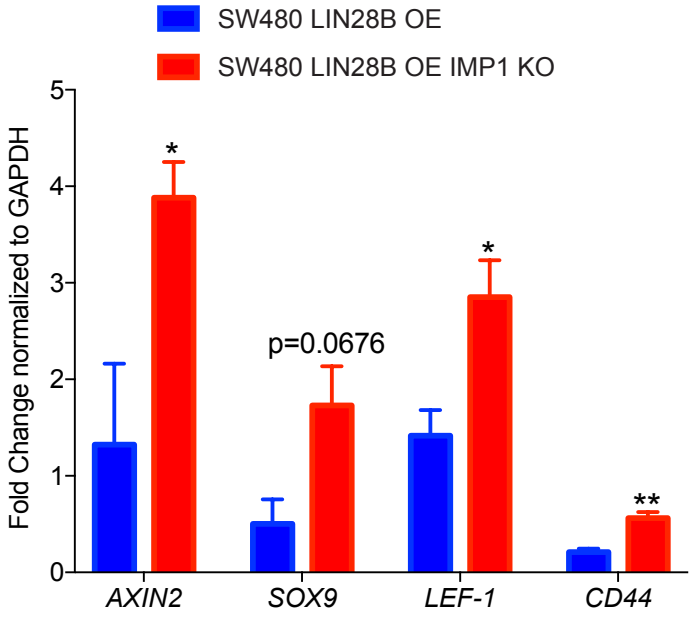

D

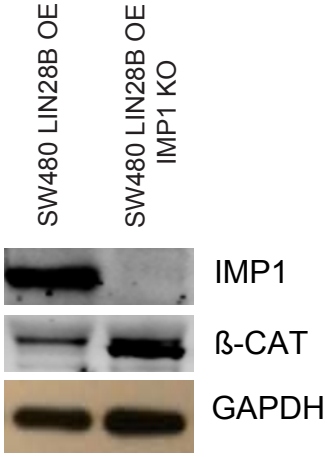

Supplemental Figure 1

A. Representative western blot demonstrating LIN28B and IMP1 expression in SW480 cells. Wild type SW480 cells express endogenous IMP1 that increases with LIN28B overexpression (OE). CRISPR-cas9-mediated deletion of IGF2BP1 (IMP1) in SW480 cells (WT and LIN28B OE). SW480 cells do not express LIN28B endogenously. **B**. Scatterplot of binding efficiencies of RNA targets of IMP1 identified by enhanced UV crosslinking and immunoprecipitation (eCLIP) (Conway et al. 2016) with differential translational efficiency of the targets identified in **1C**. We find no significant correlation between the two (R2=0.0024). **C**. qRT-PCR for Wnt target genes in SW480 cells overexpressing LIN28B with and without IMP1 deletion. (n=3 passages). Several Wnt targets are significantly upregulated with IMP1 deletion. **D**. Western blot showing ß-CATENIN increase with IMP1 deletion in SW480 cells with LIN28B overexpression. (* $p<0.05$ by Student's t-test)

Chatterji_Supplemental Figure 2

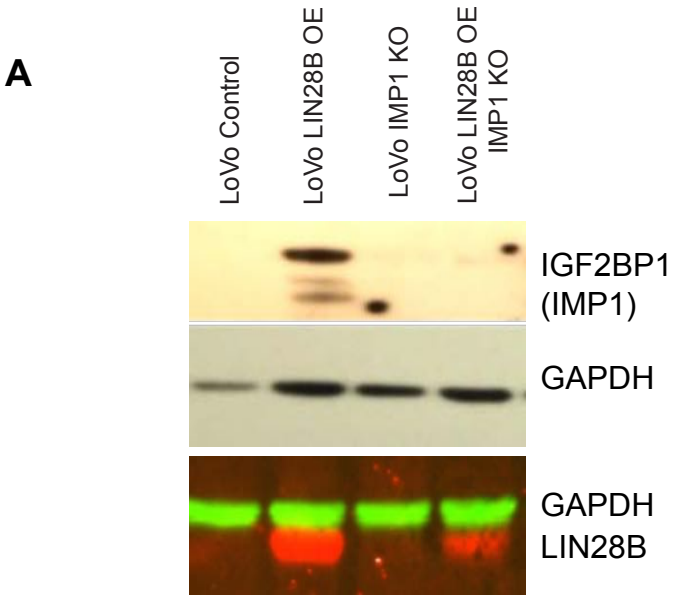

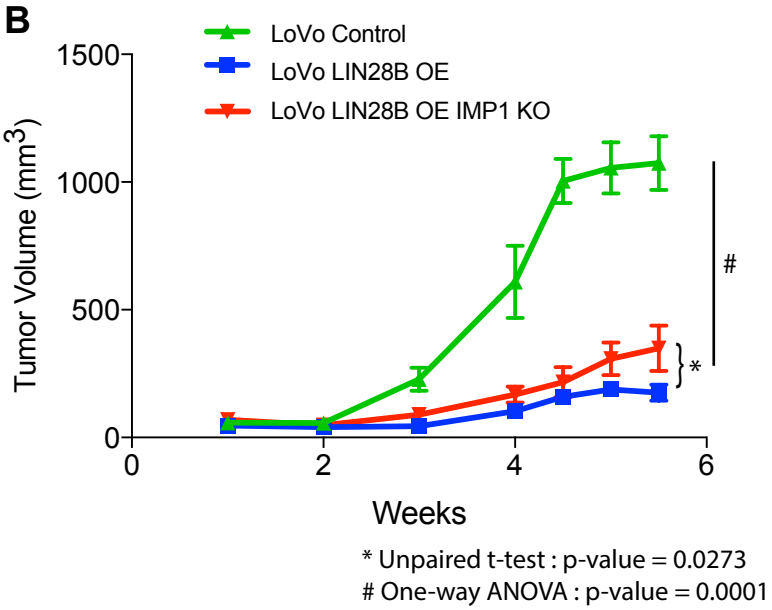

* Unpaired t-test : p-value = 0.0273
\# One-way ANOVA : p-value = 0.0001

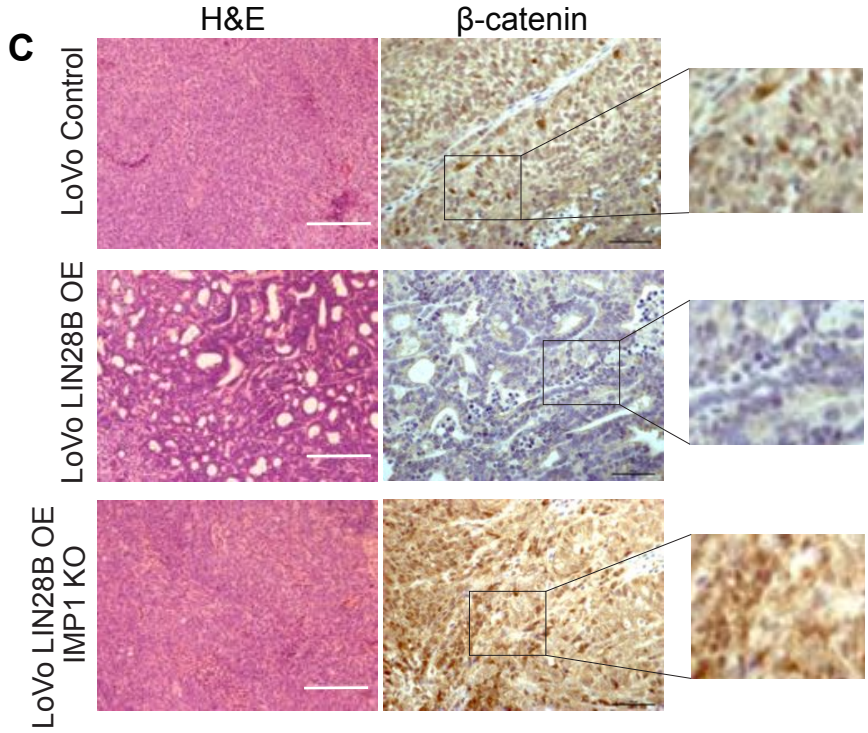

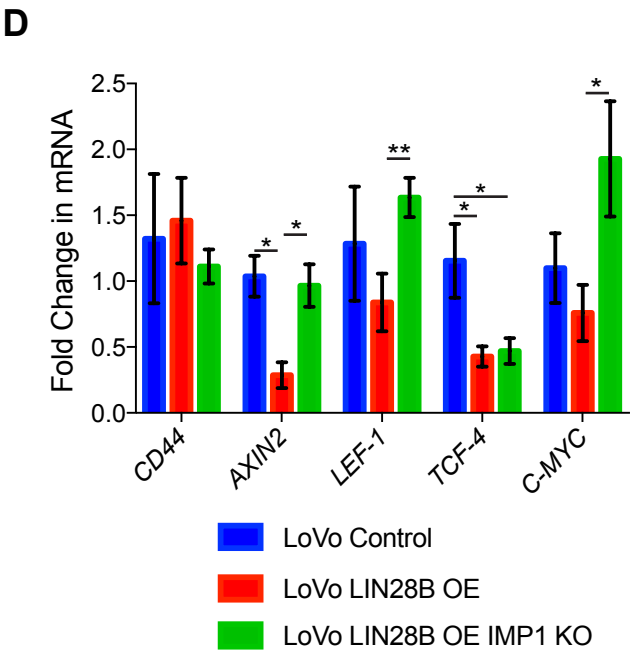

E

Total number of CRC tumors examined	228
Total number of LIN28B overexpressing tumors	37
G1 (Well-Differentiated)	5.41% (2/37)
G2 (Moderately Differentiated)	86.49% (32/37)
G3 (Poor Differentiated)	8.11% (3/37)

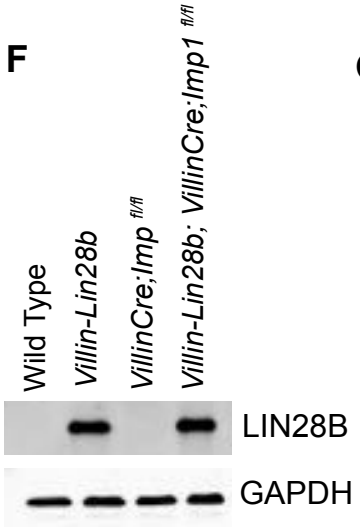

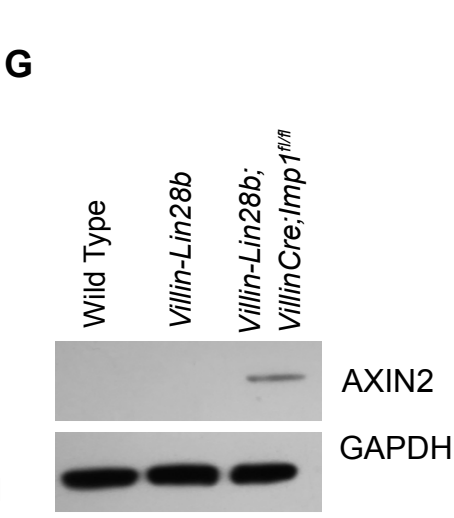

Supplemental Figure 2

A. Representative western blots demonstrating LIN28B and IMP1 expression in LoVo cells. Wild type (WT) LoVo cells show undetectable IMP1 expression that was increased with LIN28B OE. CRISPR-cas9-mediated deletion of *IGF2BP1* (*IMP1*) in LoVo cells (WT and *LIN28B* OE). **B**. Xenograft (subcutaneous) experiments with LoVo cells (n=10 per cell type) show a significant decrease in tumor size with LIN28B overexpression (169.9 ± 31.12 mm^3 at sacrifice) as compared to WT cells (1145 ± 120.3 mm^3 at sacrifice). This effect is partially rescued with IMP1 knockout (417.6 ± 107.7 mm^3 at sacrifice). **C**. Representative histological sections of the xenografts from **B** show highly differentiated tumors in LoVo cells with LIN28B overexpression. This is not observed in tumors from WT LoVo cells or LIN28B overexpressing LoVo cells with IMP1 deletion where the tumors are poorly differentiated and express more ß-catenin staining (Scale bars = 500μm). **D.** Relative expression of *Wnt* target genes in xenograft tumors from **B** (n> 4 tumors per genotype). **E**. Table showing differentiation status of LIN28B overexpressing human colorectal tumors from tumor tissue microarray (matched normal and tumor samples n=37). A majority of the tumors show increased differentiation. **F**. Representative western blot showing LIN28B expression in the intestinal epithelium of the 4 genotypes. **G**. Representative western blot showing increased AXIN2 expression in the 3D organoids/enteroids cultured from crypts of *Villin-Cre;Villin-Lin28b;Imp1*$^{fl/fl}$ mice.

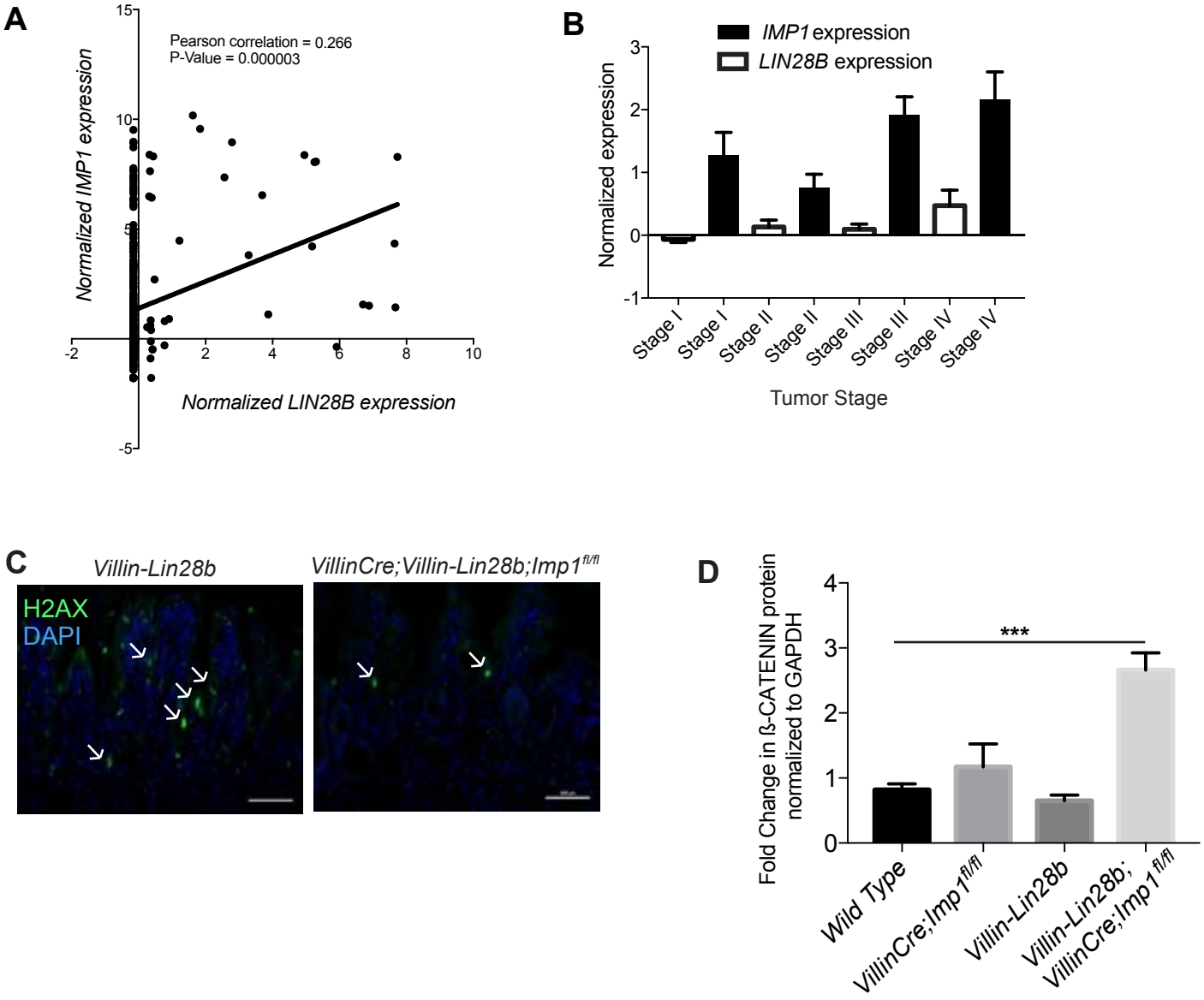

Supplemental Figure 3

A. Correlation graph between normalized mRNA expression intensities of LIN28B and IMP1 in the colon adenocarcinoma and rectal adenocarcinoma (COADREAD) datasets in the Cancer Genome Atlas (Cline et al. 2013) (n=300 patients). LIN28B expression significantly correlates positively with IMP1 expression. **B**. TCGA analysis showing LIN28B and IMP1 expressions in different stages of colorectal cancer. IMP1 is expressed highly in all four stages irrespective of LIN28B expression levels showing that IMP1 expression is potentially regulated by factors in a LIN28 dependent and independent fashion. **C**. Representative H2AX staining in *Villin-Lin28b* and *Villin-Cre;Villin-Lin28b;Imp1fl/fl* mice 4 days after 12Gy whole body radiation. Arrows indicate H2AX foci. (Scale bars = 500µm) **D**. Quantification of ß-CATENIN protein via western blots of the crypts cells of the mice of the 4 genotypes (n=3 per genotype)

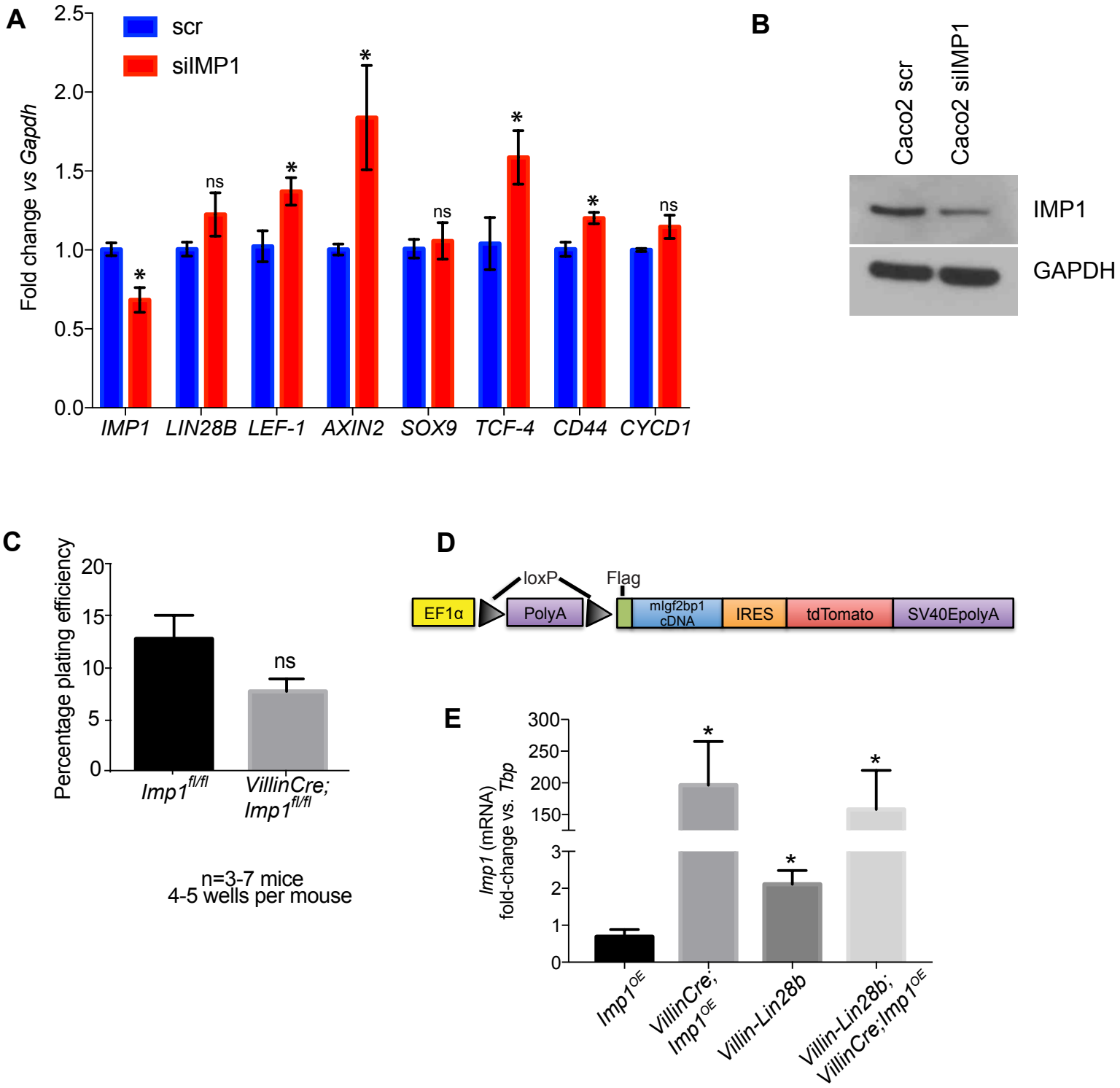

Supplemental Figure 4

A. qRT-PCR for Wnt target genes in CaCo2 cells with IMP1 knockdown as compared to controls. (n=3 independent experiments). Several Wnt targets are significantly upregulated with IMP1 knockdown. **B**. Western blot showing IMP1 knockdown using siIMP1 in CaCo2 cells

C. Enteroid plating efficiency from *Imp1 fl/fl* and *VillinCre;Imp1fl/fl* mice at homeostasis revealed no significant difference between genotypes. N=3-7 mice per genotype with 4-5 wells per mouse analyzed.

D. Construct for *Imp1OE* mice, which were then crossed with *VillinCre* mice.

E. The *VillinCre;Imp1OE* mice were verified for intestinal IMP1 expression by qRT-PCR in isolated epithelia from these mice. *P<0.05, N=3-4 mice per genotype.

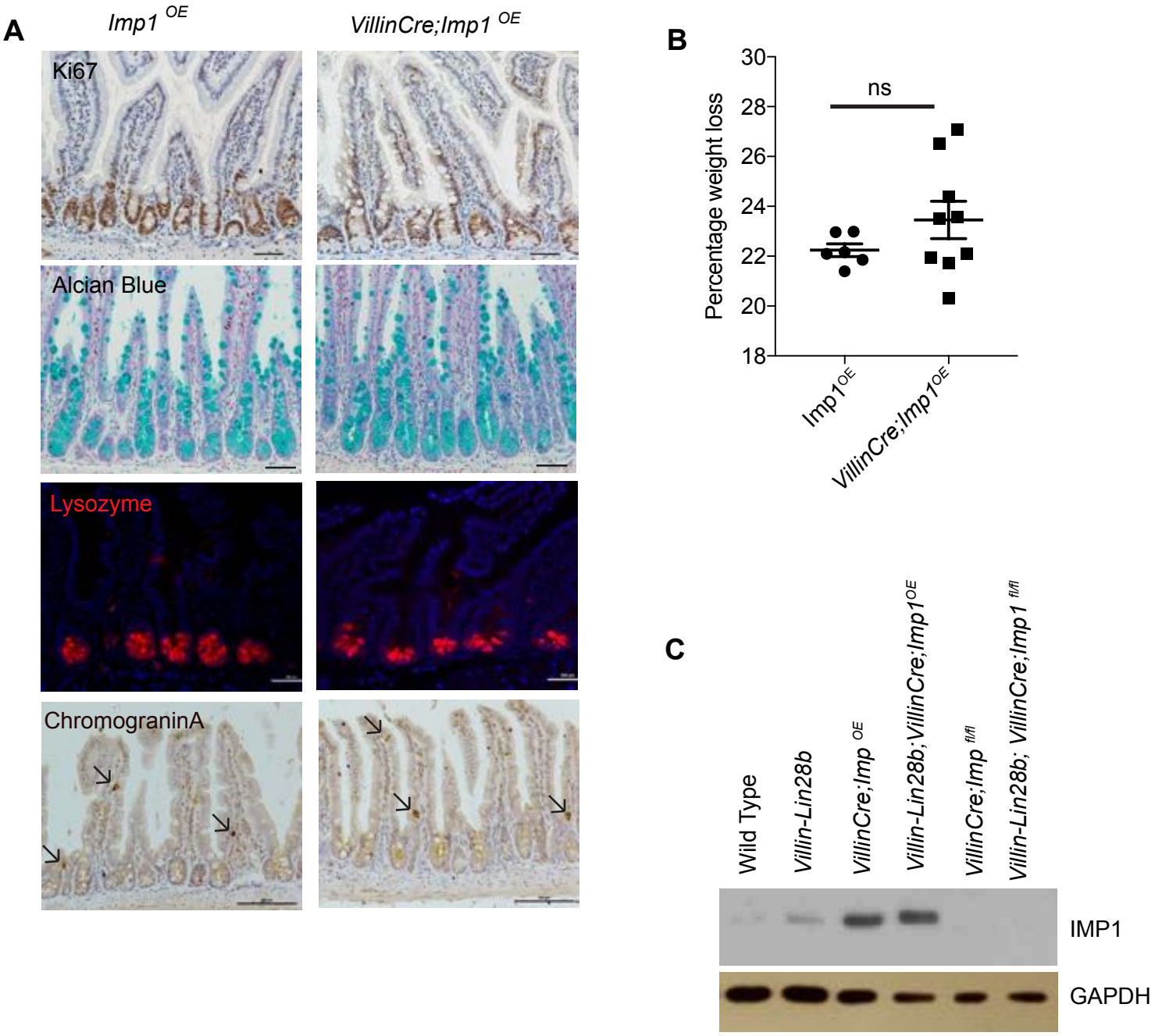

Supplemental Figure 5
A. Representative staining for Ki67 (proliferation), Lysozyme (Paneth cells), Alcian blue (goblet cells) and chromogranin A (enteroendocrine cells) in *VillinCre;Imp1*^{OE} mice as compared to controls. (Scale bars = 500µm). **B**. *Villin-Cre;Imp1*^{OE} mice lost similar weight at sacrifice following irradiation compared to *Imp1OE* controls. (23.46 ± 0.7485% mean weight loss in *Villin-Cre;Imp1*^{OE} mice (n=9) versus 22.24 ± 0.2556% in *Imp1*^{OE} (n=6)) **C**.Western Blot for IMP1 in isolated epithelia from all the genotypes .

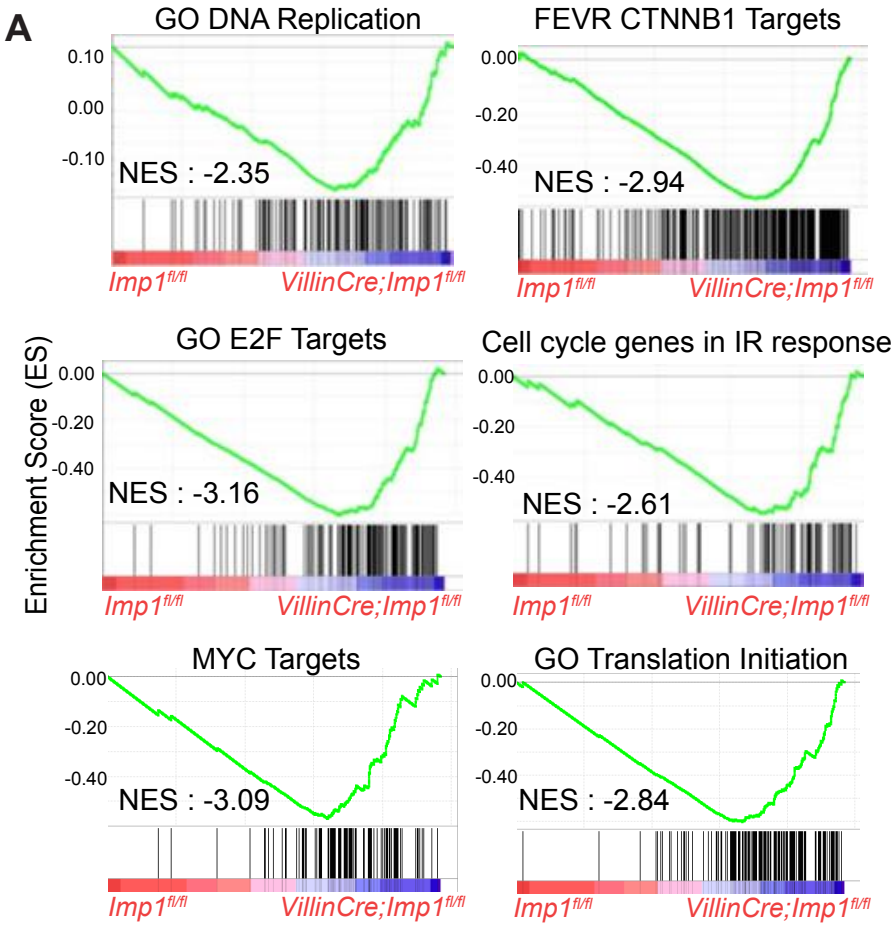

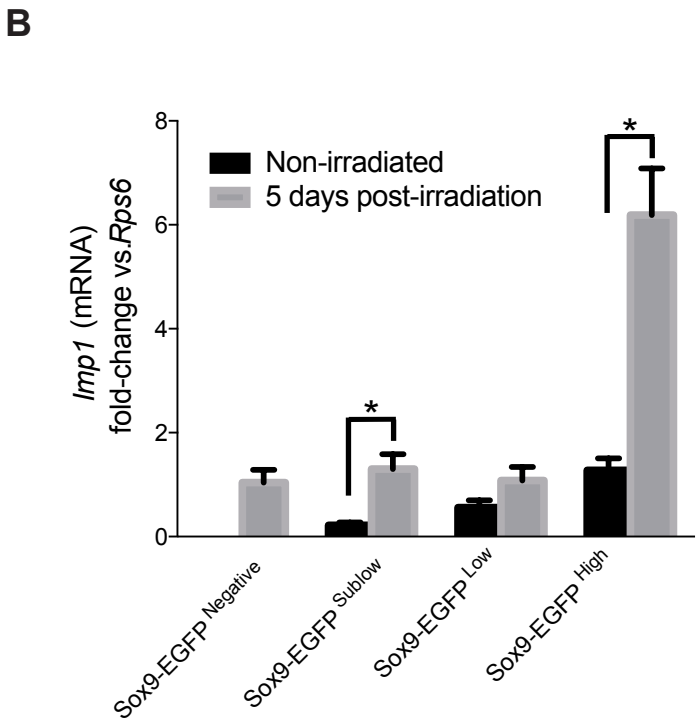

Supplemental Figure 6

A. Crypts cells from *Imp1*$^{fl/fl}$ and *VillinCre;Imp1*$^{fl/fl}$ mice were isolated and RNA-Seq performed N=3 mice per group. Gene set enrichment analysis (GSEA) revealed enrichment of gene targets involved in proliferation, regeneration and Wnt signaling in *VillinCre;Imp1*$^{fl/fl}$ mice as compared to control mice (p-value < 0.001, FDR < 0.001)
(NES = Normalized Enrichment Score; It reflects the degree to which a gene set is overrepresented at the top or bottom of a ranked list of genes).
B. Imp1 expression is upregulated in all the different *Sox9-EGFP* cell fractions five days following 14Gy irradiation and significantly upregulated in the Sublow and High populations (n=5 animals per group).